Hindawi
Shock and Vibration
Volume 2022, Article ID 7272775, 11 pages
https://doi.org/10.1155/2022/7272775

Research Article

Research on Mechanical Characteristics of Asphalt Graded Gravel Layer with Ballast Bed under Train Load

Shu Sun

TaiZhou Polytechnic College, Jiangsu, Taizhou 225300, China

Correspondence should be addressed to Shu Sun; 458809515@qq.com

Received 29 March 2022; Revised 6 July 2022; Accepted 22 August 2022; Published 15 September 2022

Academic Editor: Yun-Lai Zhou

This article carries out laboratory tests, driving tests, and discrete element method simulations to study the mechanical properties of ballasted tracks including asphalt graded gravel and the influence of factors such as the thickness of asphalt graded gravel layer and train speed on the dynamic characteristics of the closed structure of asphalt graded gravel. It was discovered that the asphalt graded gravel can improve the bearing capacity of the ballasted track subgrade structure and improve the stability of the ballast bed. Comparative analysis shows that as the depth of the ballast bed increases, the amplitude and frequency of the velocity fitting function of each layer gradually decrease. Appropriately increasing the depth is beneficial to the stability of the ballast bed; the vertical dynamic deformation and dynamic stress decrease with the increase of the thickness of asphalt graded gravel layer; with the increase of train speed, the peak frequency of the corresponding spectrum of asphalt graded gravel layer acceleration increases. There are currently few research studies on the asphalt graded crushed stone structure laid in the ballast bed, especially the mechanical properties of the asphalt graded crushed stone structure laid by the discrete element simulation are still blank. The acceleration of the asphalt graded gravel layer increases corresponding to the peak frequency of the spectrum. The peak frequency of the acceleration response of the asphalt graded gravel layer increases. The research rules can provide a reference for the research and development of shock absorption equipment. The research results of this article can provide technical support for the application of asphalt graded gravel in railway engineering.

1. Introduction

As a traditional track structure, the ballast bed has the characteristics of good drainage, low cost, and easy maintenance. It has become one of the important ways of passenger transportation and bulk cargo transportation in the world. However, as the service time increases, the granular structure will deform as the number of train loads increases [1], which will cause accelerated damage, deterioration, and dirt to the ballast track structure and will eventually lead to problems such as a large amount of line maintenance, high maintenance costs, and driving unsafety [2].

The combination of engineering experimental data and discrete element simulation shows that the asphalt graded crushed stone structure has excellent mechanical bearing performance, which can significantly improve the stress state of the subgrade structure and the vibration characteristics of the track-subgrade system. The optimization of the subgrade structure has created favorable conditions, and this paper also provides a new technical idea for enriching the research of ballast bed and subgrade structure.

At present, to improve the service performance of the ballast bed, a large number of technical studies have been carried out at home and abroad. To improve the bonding force between the ballast particles, polyurethane (ballast glue) curing technology is used to strengthen the granular structure to improve the rigidity and stability of bridges, tunnels, and ballastless ballasted transition sections [3].

Some laboratory tests use geogrids to reinforce the ballast bed, so that selflocking phenomenon can occur between the ballast particles in the ballast bed, thereby improving the cohesion and friction angle of the granular ballast bed [4]. By laying small particles of stone on the 40 m long section of the Shuohuang Railway, the ballast and the

surface of the subgrade can be efficiently sealed, which can effectively solve the problem of compaction caused by the intrusion of the surface of the subgrade into the ballast. Combined with polyurethane curing technology, it can be widely used in the ballast road section which needs special reinforcement.

To improve the overall mechanical performance of ballast bed, China has successively laid full-face asphalt graded crushed stone test sections on Zhengzhou-Xuzhou, Wuhan-Huanggang, Beijing-Zhangjiakou, Zhengzhou-Wanzhou, and other lines, which greatly improves the waterproof performance and mechanical properties. There are no problems such as frost heave and thawing settlement, mud tumbling, and bed softening [5]. However, the full-face asphalt graded gravel layer is only applied to the ballastless track section. Research and application of ballasted track sections are inadequate [6]. Therefore, this article analyzes the laboratory tests and in situ tests and uses the discrete element method to establish a simulation model of sleeper-ballast-asphalt graded gravel-subgrade to study the mechanical properties of the ballast bed under the difference in asphalt graded gravel thickness and train speed.

2. Validation of Ballast Bed Model

In this article, the discrete element method analysis software is used to establish the asphalt graded gravel model and the ballast bed model with multiple sleepers. Meso-parameters of the discrete element model are calibrated by data obtained from the laboratory uniaxial compression test and the in situ ballast bed test. Specifically, the laboratory uniaxial compression test is used to calibrate the microscopic parameters of the asphalt graded gravel model, and the in situ ballast bed resistance test is used to calibrate the microscopic parameters of the ballast particles. The different meso-parameters are used to comprehensively simulate the physical properties of the different components of the ballast bed.

2.1. Verification of Asphalt Graded Gravel Layer. In this article, the uniaxial compressive strength of asphalt graded gravel samples is measured. Cylinders with a diameter of 50 mm ± 1 mm and a height of 100 mm ± 1 mm are prepared as shown in Figure 1 [7]. Under unconfined conditions, at the temperature of 15°C, the axial stress-strain curve is obtained by continuous loading until the specimen fails [8].

This article selects AC-16 asphalt graded gravel, and the grading curve is shown in Figure 2 [7]. The figure shows the screening of mineral powder, 0-5 mm, 5-10 mm, and 10-20 mm diameter gravel in asphalt graded gravel. The discrete element simulation model is established using synthetic gradation [9].

The size of the discrete element model established in this section is 50 mm in diameter and 100 mm in height. Due to the calculation limitation of PFC2D software, ore powder and crushed stone with a diameter of 0-5 mm are defined as fine aggregates. The fine aggregate is established by the ball element, and the particle size of the ball element is uniformly simplified to 0.5 mm. The number of ball elements is 4427. The crushed stone with a diameter of 5-10 mm and 10-20 mm is defined as coarse aggregate, and the coarse aggregate is established by the clump element. The number of clump elements is 912. Wall elements are generated above and below the model, and uniaxial loading is achieved by applying velocity loads to the wall elements.

To simulate the physical and mechanical properties of the asphalt graded gravel, it is necessary to accurately select the discrete element contact model. According to the discrete element software PFC, there are two built-in bonding models [10]: linear parallel bond model and linear contact bond model. Linear parallel bond model can change the length of the bonding gap between particles to adjust the state of the structure and can transmit forces and moments, so that the linear parallel bond model is adopted between asphalt mortar and between mortar particles and coarse aggregate. For the linear contact bond model, it can only transmit forces but not moments. This constitutive model can well simulate the mechanical properties of the thin asphalt mortar layer between coarse aggregates. Reference [11] explains the working principles of the two models in detail [12]. Figure 3 shows the discrete element method simulation model established [7].

The compression test is carried out by the established discrete element simulation model, and the stress-strain curve detected by uniaxial compression of this model according to the laboratory test loading conditions is shown in Figure 4 [7]. Fitting the stress-strain curve and analyzing its correlation, the peak compressive strength is 5.42 MPa (the peak compressive strength of laboratory test is 5.37 MPa). Analyzing the test stress-strain curve and the simulated stress-strain curve before and after reaching the peak, this article adopts a two-stage equation fitting function expression with the peak compressive strength as a dividing point. The basic equations of the function are $\sigma = A\varepsilon + B\varepsilon^2 + C\varepsilon^3$ (growth segment) and $\sigma = 1/\varepsilon^m$ (reduce segment). According to this function, the stress-strain function expressions before and after the peak are established and their correlation is calculated. The results are shown in Table 1 [13].

According to the fitting results and the comparison diagram of test and simulation, the stress-strain correlation between the experimental curve and the simulation data before and after the peak is 0.994 and 0.957, respectively. The fitted function can well reflect the change of stress with strain during the loading process [7]. The test and simulation results are significantly correlated, and the various meso-parameters in the discrete element model can correctly characterize the mechanical properties of asphalt graded gravel.

2.2. Verification of the Ballast Layer of the Ballasted Bed. Parameters of ballast particles are calibrated based on the longitudinal resistance data of the ballast bed measured on-site [14]. Testing the longitudinal resistance of the ballast bed requires the use of hydraulic jacks, force sensors, and reaction support. Hydraulic jacks provide longitudinal thrust that causes longitudinal displacement of sleepers, and the

Figure 1: Uniaxial compressive strength test.

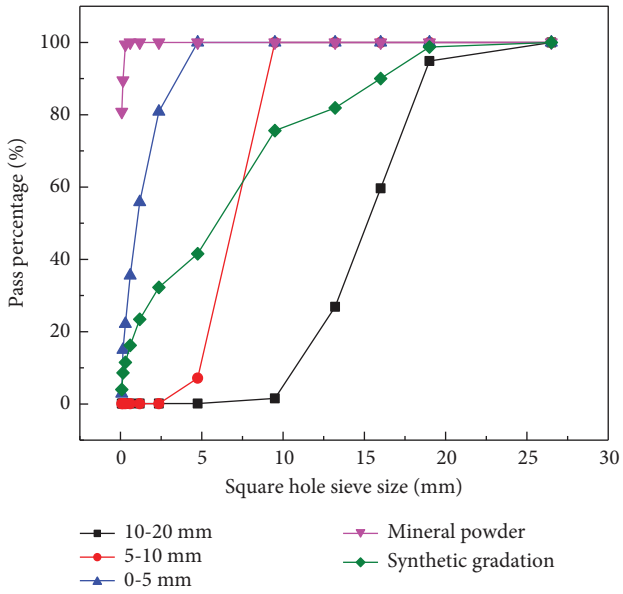

Figure 2: Gradation of asphalt gravel.

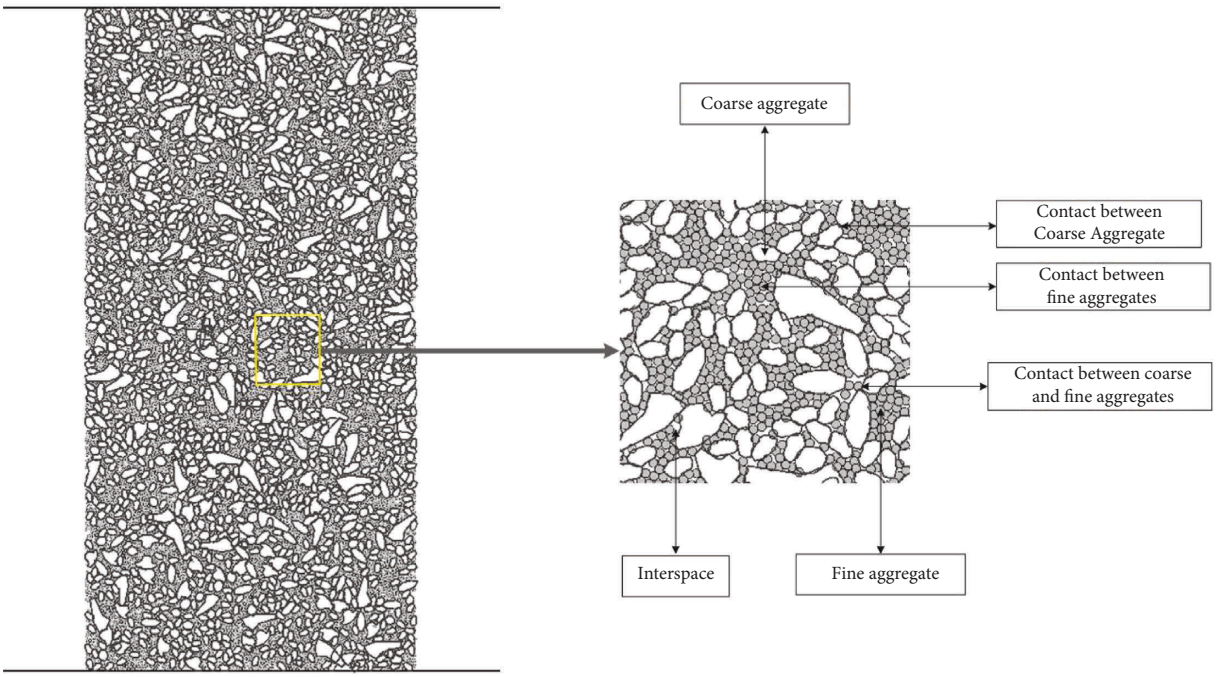

Figure 3: Discrete element method model of asphalt graded gravel.

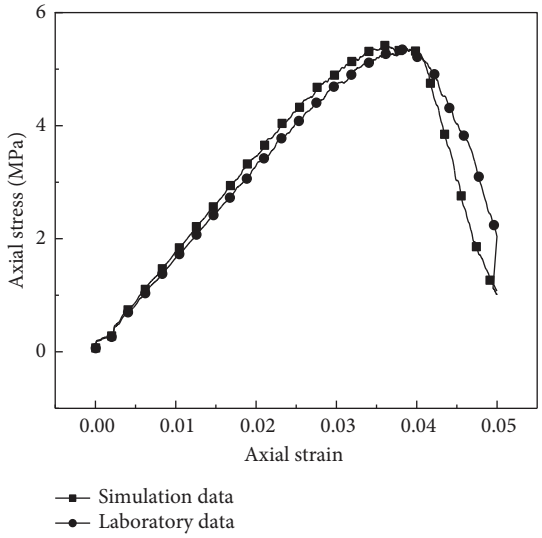

Figure 4: Uniaxial compression test and simulation comparison.

Table 1: Uniaxial compression test and simulation fitting function.

Category	Condition	Fitting formula	Correlation R^2
Before the peak	Laboratory data	$\sigma = 88195\varepsilon - 1.32\varepsilon^2 + 5.78\varepsilon^3$	0.994
	Simulation data	$\sigma = 88217\varepsilon - 1.21\varepsilon^2 + 5.72\varepsilon^3$	
After the peak	Laboratory data	$y = 1/x^{1.14}$	0.957
	Simulation data	$y = 1/x^{1.18}$	

displacement is measured by a dial gauge. The force sensor is closely installed on the jack, detecting real-time resistance data and transmitting to the digital display for reading, to obtain the longitudinal resistance-displacement curve. The on-site measurement and test principle are shown in Figures 5 and 6.

The discrete element analysis software is used to establish a simulation model including sleepers, subgrade, and asphalt graded gravel. Based on the longitudinal resistance-displacement data of the ballast bed measured in the in situ test, the two-dimensional sleeper-ballast discrete element model in this article is established in full scale according to the "High-speed Railway Design Code" [15]. The sleeper adopts the new type III concrete sleeper, with a sleeper spacing of 0.67 m, a sleeper buried depth of 0.185 m, and a ballast layer thickness of 0.3 m. The particle size of the ballast is set according to the special grade gravel ballast gradation.

The sleeper in the discrete element model is built using the clump element in the PFC. Firstly, according to the cross-sectional size of the sleeper, use AutoCAD software to draw, and export the file in DXF format, then import it into PFC2D through the "geometry import" command, and then fill in the imported geometry through the "clump template create" command. Finally, generate 7 sleeper models in the model through the "clump replicate" command. As a kind of entity in PFC, the clump can be assigned parameters such as density, stiffness, and friction coefficient to meet the simulation requirements of sleepers.

The ballast model is generated by the irregular elements according to the gradation, and the irregular shape is

Figure 5: On-site measurement diagram.

randomly generated by the AutoCAD software and imported into the PFC for modeling. The ballast particle gradation table is shown in Table 2.

The ballast model adopts 5 kinds of irregular shapes. As shown in Figures 7 and 8, a total of 8633 ballast particles are generated.

The asphalt layer model is established according to Section and generates 22425 asphalt layer particles. The subgrade model is composed of ball element. The subgrade adopts the conventional soil parameters in the PFC to generate 7177 subgrade particles. Due to computational constraints, the model cannot be infinitely long, so the

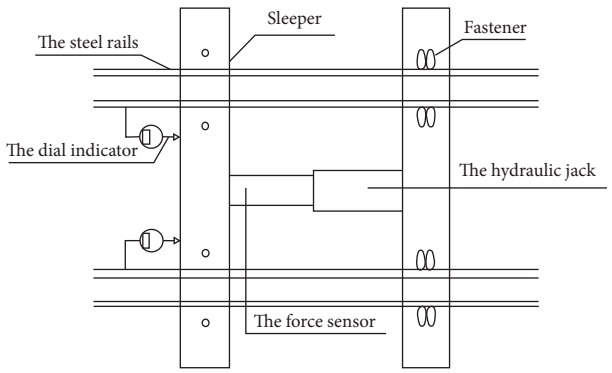

Figure 6: Test principle diagram.

Table 2: Ballast particle gradation.

Square hole mesh length (mm)	22.4	31.5	40	50	60
Pass sieve mass percentage (%)	3	25	65	99	100

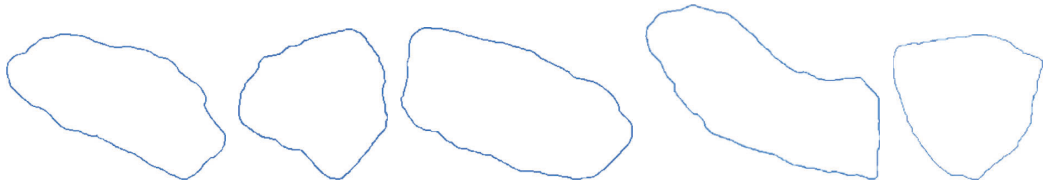

Figure 7: Ballast particle shape.

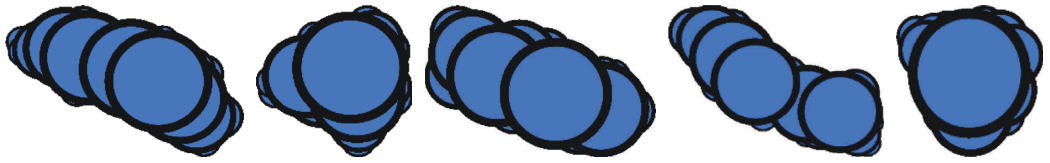

Figure 8: Ballast model.

boundary needs to be set. The wall damping boundary is commonly used in PFC. This model needs to set the damping coefficient for the boundary wall to absorb the energy transferred, and the damping coefficient is set to 0.8. The discrete element model of ballast bed established by PFC is shown in Figure 9 [7].

By applying a constant speed of 1 mm/s to the right of the middle sleeper in the model, the sleeper will slide under the action of external force. Monitor the force-displacement curve of the sleeper during this process and compare it with the in situ test results to verify the validity of the meso-parameters of the discrete element model of the ballast. Besides, according to the literature, the relationship between the resistance of the ballast bed and the displacement is generally a power function relationship. Therefore, the measured curve and the simulation curve are fitted with a power function to reflect their correlation. The power function relationship is shown in the following formula:

$$Q = Q_0 - By^Z + Cy^{1/N}, \quad (1)$$

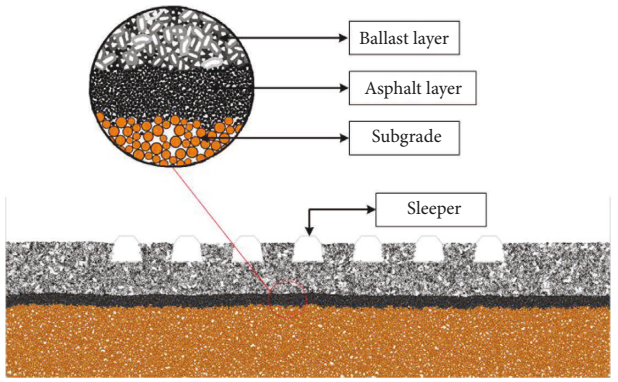

Figure 9: Discrete element model diagram of ballast bed.

where Q_0 is the initial longitudinal resistance of the ballast bed (kN), y is the longitudinal displacement of sleepers (mm), B, C, Z, and N are resistance coefficients, and N is taken as 4/3 in the literature [16].

Fitting results: measured data is $Q = 8.59 - 17.55y + 30.01y^{3/4}$ and simulation data is $Q = 2.63 - 13.01y + 27.26y^{3/4}$.

It can be seen from Figure 4 and the longitudinal resistance-displacement fitting function relationship that the correlation coefficient between the discrete element model and the measured significance test on-site is 0.925. Hence, the ballast-sleeper model established in this article can well reflect the relationship between the longitudinal resistance of the ballast bed and the lateral displacement of the sleeper. The meso-parameters of the ballast and sleepers in this model can accurately simulate the contact relationship in the real situation. The meso-parameters obtained from the model verification in this section are shown in Table 3.

3. Analysis of Influencing Factors of Mechanical Properties of Asphalt Graded Gravel Layer

3.1. The Influence of Asphalt Graded Gravel Layer Thickness. The thickness of the asphalt graded gravel layer in the ballasted track has an impact on the changes in the overall structural mechanical properties, the closed ballast, and the subgrade. The appropriate thickness of the asphalt graded gravel layer can greatly improve the dynamic characteristics of the ballast bed. [17] This article selects 3 different thicknesses, which are 8 cm, 16 cm, and 24 cm, and uses the meso-parameters calibrated above to study the influence of asphalt graded gravel layer thickness on the dynamic response.

Reference pointed out that the contact stress between the sleepers and the ballast during the operation of the train is 370 kPa [18]. Considering the contact area between the sleeper and the ballast in this model, the contact force between the sleeper and the ballast can be calculated to be 118.4 kN (370 kPa ∗ 0.32 m ∗ 1 m). The dynamic action of the train is simulated by applying a sinusoidal load to the sleepers in the model. The sinusoidal load function is expressed as follows:

$$F(t) = F_0\left(-1 - \sin\left(2\pi f t - \frac{\pi}{2}\right)\right), \quad (2)$$

where F_0 is the half-peak value of the force, which is 60 kN in this article;f is the frequency, this article uses 10 Hz; and t is time.

The contact force distribution between sleepers and ballast particles during loading and unloading is shown in Figures 10 and 11. The contact force is characterized by the thickness of the force chain. The simulation results indicate that the maximum contact force is mainly concentrated near the bottom surface of the sleeper. The cone-shaped distribution enables the ballast to better withstand the load from the sleeper. During the entire loading process, ballast particles will dislocate, move, and then deform [19].

After applying the above load to the sleeper, we select the middle part of the sleepers, ballast layer, asphalt gravel layer, and subgrade for monitoring. The velocity response of the three train loading cycles is monitored. The speed relationship of each layer is shown in Figure 12 [7]. The speed curve form of each layer under load is basically the same as the above load function relational expression, so this article fits and obtains the velocity relational expression of each layer under load according to the function relational expression. The expression is shown in Table 4.

Table 3: Model meso-parameters.

Parameter type	Parameter name	Value
Ballast particles	Normal stiffness (ball-ball) kn ($MN{\cdot}m^{-1}$)	550
	Shear stiffness (ball-ball) ks ($MN{\cdot}m^{-1}$)	550
	Normal stiffness (ball-facet) ($MN{\cdot}m^{-1}$)	900
	Shear stiffness (ball-facet) ($MN{\cdot}m^{-1}$)	900
	Density ($kg{\cdot}m^{-3}$)	2400
	Friction coefficient (ball-ball)	0.5
	Friction coefficient (ball-facet)	0.7
Asphalt particles	Normal stiffness (ball-ball) pb_kn ($MN{\cdot}m^{-1}$)	1000
	Shear stiffness (ball-ball) pb_ks ($MN{\cdot}m^{-1}$)	5000
	Friction coefficient (ball-ball)	0.5
	Normal critical damping ratio dp_nratio	0.5
	Shear critical damping ratio dp_sratio	0.5
	Tensile strength pb_ten (MPa)	100
	Cohesion pb_coh (MPa)	500

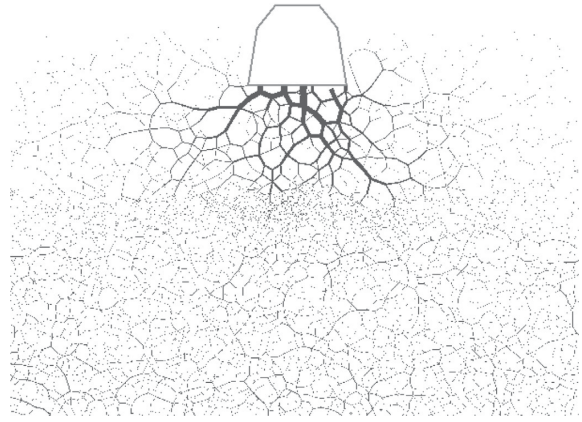

Figure 10: Loading force chain diagram.

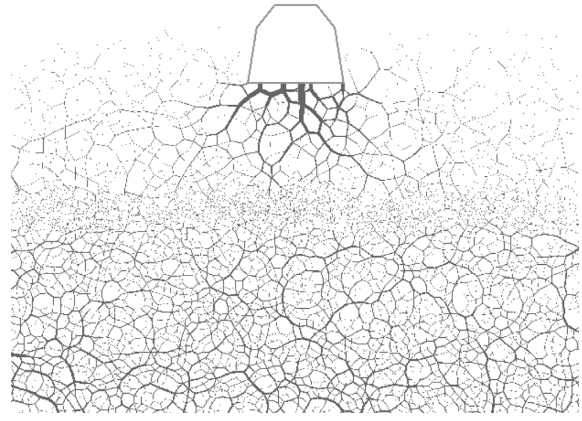

Figure 11: Unloading force chain diagram.

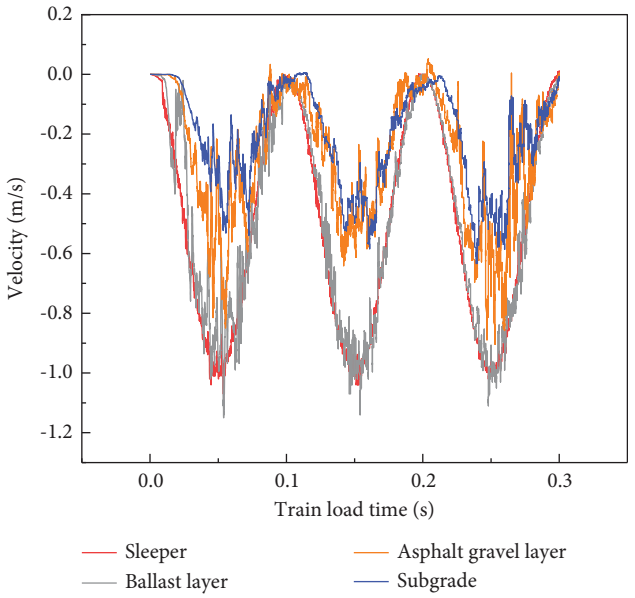

Figure 12: Velocity time history curve of each layer of ballasted track.

Through the analysis of the above detection curves, it can be seen that in the longitudinal dimension, the ballast layer, the asphalt graded gravel layer, and the subgrade all have a certain degree of attenuation, and the resulting velocity peaks are 1.15 m/s, 0.89 m/s, and 0.65 m/s. The attenuation rates are 22.6% and 26.6% in turn. Table 4 lists the velocity time history relationship of each layer under the excitation of the train load. We found that as the depth increases, the amplitude and frequency of the speed function of each layer gradually decrease. Therefore, it can be concluded that the depth of the ballasted track is one of the important indicators to maintain the stability of the mechanical properties of the ballast bed.

3.2. Analysis of Vertical Dynamic Deformation. By extracting the calculation results of the vertical dynamic deformation under the asphalt graded gravel thickness of 8 cm, 16 cm, and 24 cm, the vertical dynamic deformation is analyzed with the thickness of the asphalt graded macadam layer. Figure 13 shows the relationship between the vertical dynamic deformation of each layer and the thickness of the asphalt graded gravel layer.

As is shown in Figure 13, when the asphalt graded gravel layer closed structure with the same thickness is laid, the vertical displacement of the ballast layer, asphalt gravel layer, and subgrade layer gradually decreases from the top to the bottom. Specifically, the vertical dynamic displacement of each layer corresponding to the thickness of 8 cm is 4.53 cm, 2.58 cm, and 1.69 cm, respectively, to the thickness of 8 cm is 4.23 cm, 2.48 cm, and 0.71 cm, and to the thickness of 24 cm is 4.02 cm, 2.62 cm, and 0.69 cm. It can be found that the vertical dynamic deformation of the ballast bed and the asphalt gravel layer decreases as the thickness of the closed structure of the asphalt graded gravel increases. Additionally, as the thickness increases, the vertical deformation does not decay linearly with the thickness of asphalt graded gravel. The attenuation rate will decrease with the increase in thickness. Taking the ballast layer as an example, when the thickness of the asphalt graded gravel is increased from 8 cm to 16 cm and 24 cm, the reduction ratios are 6.6% and 4.9%, respectively. It can be concluded that an appropriate increase in the thickness of the asphalt graded gravel can effectively reduce the settlement of the ballast bed and reduce the maintenance workload.

3.3. Vertical Dynamic Stress Analysis. By extracting the calculation results of the vertical dynamic stress at the thickness of 8 cm, 16 cm, and 24 cm asphalt gravel layer, the variation of the vertical dynamic stress with the thickness of the asphalt gravel layer is analyzed. Figure 14 shows the relationship between the vertical dynamic stress of each layer and the thickness of the asphalt layer.

Under the action of the train load, the local vertical dynamic stress peaks of the ballast layer, asphalt gravel layer, and subgrade layer under the thickness of 8 cm, 16 cm, and 24 cm are 0.32 MPa, 1.26 MPa, and 1.64 MPa (8 cm); 0.24 MPa, 0.97 MPa, and 1.79 MPa (16 cm); and 0.12 MPa, 0.78 MPa, 1.72 MPa (24 cm), respectively, It can be found that the vertical dynamic stress of the ballast bed and the asphalt gravel layer decreases with the increase of the thickness of the closed structure of the asphalt graded gravel, but the vertical dynamic stress of the subgrade does not change much.

When the thickness of the asphalt graded gravel layer is increased from 8 cm to 16 cm and 24 cm, the vertical dynamic stress is reduced by 25% and 50%, respectively. When the thickness of the asphalt graded gravel layer reaches 16 cm, the vertical dynamic stress of the ballast layer of the superstructure will be greatly attenuated. It can be seen that appropriately increasing the thickness of the asphalt gravel layer can improve the mechanical state of the ballast structure above the ballast bed.

3.4. Influence of Train Speed Grade. When the train speed increases, due to factors such as track irregularity, slope, and curve radius [20], the vertical load acting on the ballast bed will dynamically change, and the dynamic response transmitted to the lower part of the structure will also change accordingly. It is necessary to analyze the influence of different train speeds on the dynamic response characteristics of asphalt graded gravel layer and related structures. The export file of the in situ measured data at the driving test site is "vertical load data. txt" [21]. The vertical force time history curves of 80 km/h, 120 km/h, and 160 km/h detected by the driving test in this article are shown in Figure 15.

The driving test is to arrange a pressure sensor on the side of the track rail in service to monitor the load applied to the track during the operation of the vehicle. By monitoring this load, a series of working condition data are obtained, and these load data are applied as input parameters to the sleepers in the model to study the effect of different train speeds on the ballast bed.

Table 4: Fitting relationship of the velocity time history curve of each layer.

Monitoring location	Fitting function expression	R^2
Sleeper	$F(t) = 0.49 * (-1 - \sin(2\pi * 9.95 * t - \pi/2))$	0.997
Ballast	$F(t) = 0.44 * (-1 - \sin(2\pi * 9.55 * t - \pi/2))$	0.917
Asphalt gravel	$F(t) = 0.26 * (-1 - \sin(2\pi * 9.37 * t - \pi/2))$	0.908
Subgrade	$F(t) = 0.16 * (-1 - \sin(2\pi * 8.89 * t - \pi/2))$	0.907

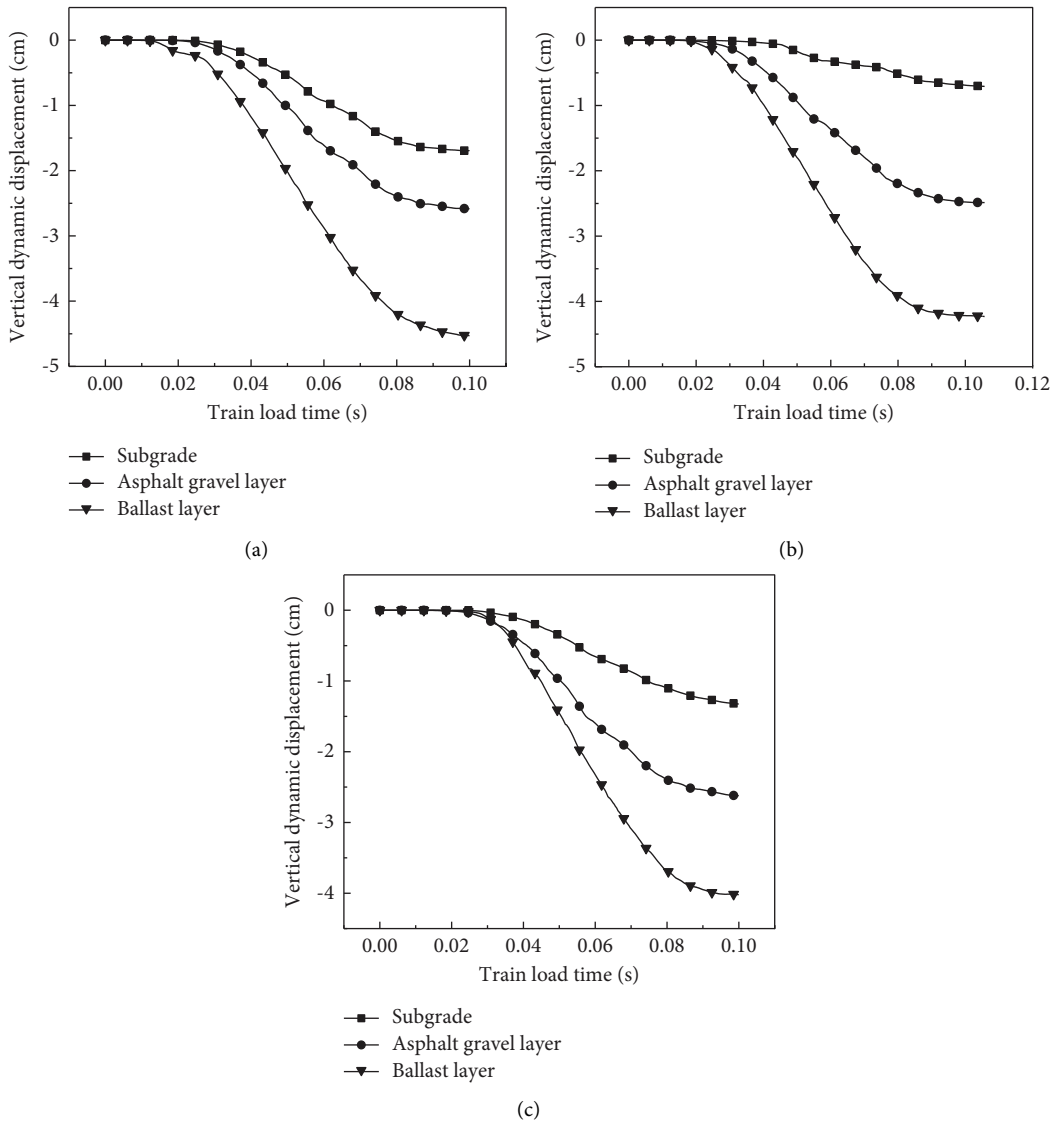

Figure 13: Vertical dynamic deformation of different asphalt graded gravel thickness: (a) 8 cm thick asphalt graded gravel, (b) 16 cm thick asphalt graded gravel, and (c) 24 cm thick asphalt graded gravel.

The vibration acceleration generated by the load of the train at each structural position of the ballast bed is one of the important indicators to measure the stability of the ballast bed [22]. Based on the 16 cm thick asphalt graded gravel model, three measured data of different driving speeds are input into the model, as load excitation is applied to the model sleepers. Taking the vibration acceleration of the ballast layer as the research object, the acceleration frequency spectrum is extracted through Fourier transform [23] and is shown in Figures 16(a)-16(c). Dynamic response characteristics of ballast bed structure under different train speeds are analyzed.

Analyzing the acceleration spectrum waveforms of the ballast at the three speed levels of 80 km/h, 120 km/h, and 160 km/h, the acceleration response spectrum of the ballast shows a single peak trend, and the peak frequencies are 1089 Hz, 2669 Hz, and 3188 Hz. The peak values of acceleration amplitude are 15.21 g, 17.71 g, and 24.57 g. It can be seen that with the continuous increase of the train speed, the peak frequency and the acceleration peak become larger, and the vibration acceleration spectrum of the ballast layer is concentrated at 0-3000 Hz. Since fasteners and sleepers have their own natural frequencies, when the vibration frequency of the

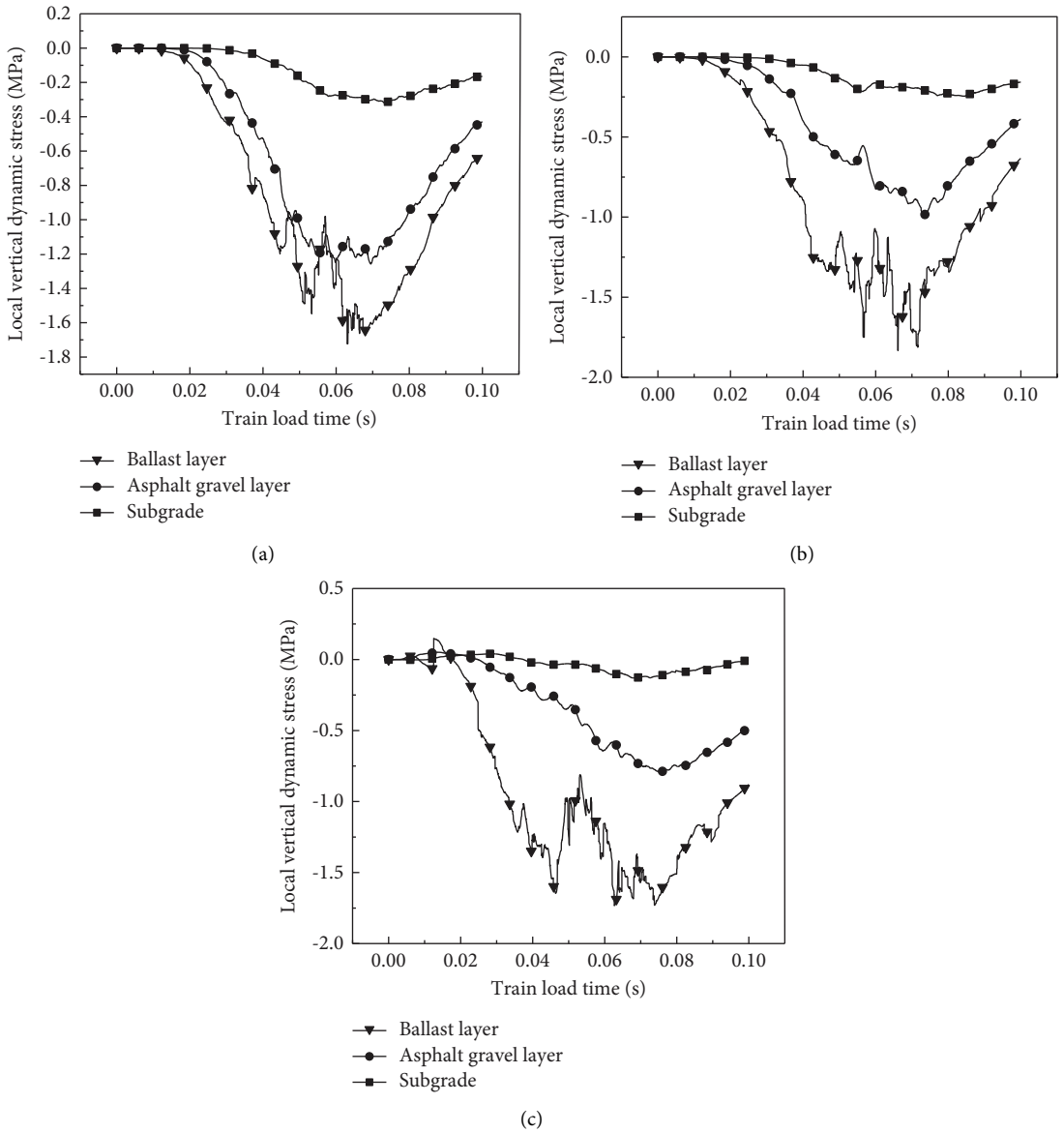

Figure 14: Vertical dynamic stress of different asphalt graded gravel thickness: (a) 8 cm thick asphalt graded gravel, (b) 16 cm thick asphalt graded gravel, and (c) 24 cm thick asphalt graded gravel.

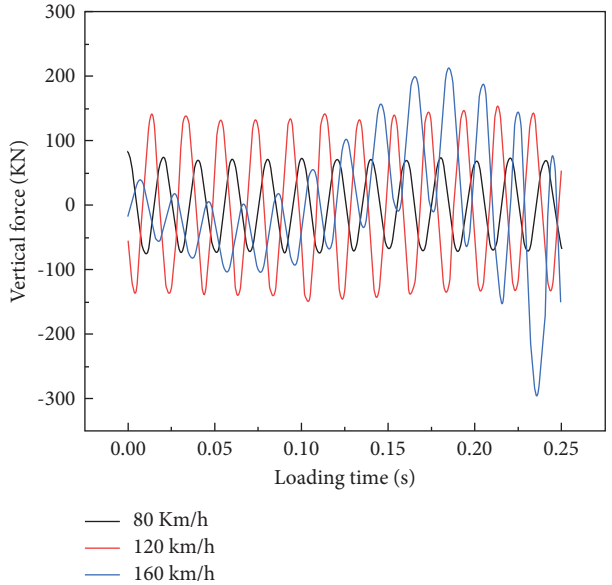

Figure 15: Vertical force of different train speed grades.

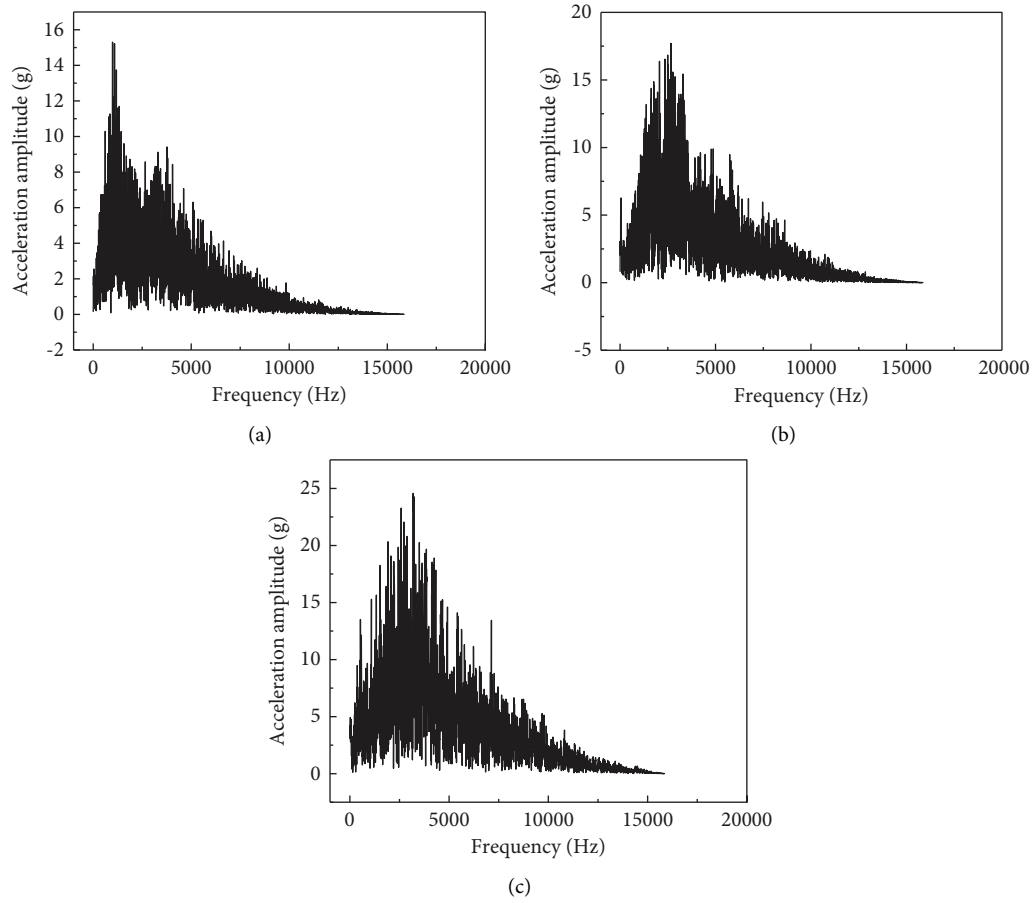

Figure 16: Acceleration spectrum of ballast layer of different speed grades: (a) 80 km/h driving speed, (b) 120 km/h driving speed, and (c) 160 km/h driving speed.

ballast is close to the natural vibration frequency of fasteners, sleepers, and other equipment, resonance may occur, resulting in accelerated deterioration of the state of the ballast bed. Therefore, the research content of this section aims to find out the vibration frequency of ballast, so that the natural vibration frequency can be controlled to achieve vibration reduction when designing fasteners, sleepers, and other equipment. The research law can provide reference for the damping design of sleepers and fasteners.

4. Conclusion

The material properties of asphalt graded crushed stone are obtained for the first time through indoor experiments, railway running test, and discrete element simulation, and some mechanical indicators that cannot be monitored through experiments are analyzed and analyze the law according to the monitoring data The main conclusions are as follows:

(1) Combining the laboratory tests and in situ test data, the established discrete element numerical model of sleeper-ballast-asphalt graded gravel-subgrade can well simulate the mechanical properties of the ballasted bed, which can provide reference for the numerical model of the gravel ballast bed with asphalt graded gravel.

(2) The laying of asphalt graded gravel can significantly reduce the vertical dynamic deformation and vertical dynamic stress of the ballast bed, but it mainly affects the superstructure such as the ballast layer, and the subgrade changes little. The main reason is that the asphalt gravel material has certain cohesiveness, which can improve the overall strength of the granular structure and separate the ballast from the subgrade, thereby inhibiting the relative displacement between the ballast particles.

(3) Obtain the vertical force through the driving test, and obtain the ballast acceleration response frequency range and acceleration amplitude at different train speeds. The two indicators are proportional to the driving speed. The change law and simulation value can be the corresponding speed of the ballast bed shock absorption for reference.

Data Availability

The basic data of the research results are based on the test results of our laboratory tests and field tests and can be uploaded as data later if necessary.

Conflicts of Interest

The author(s) declared no potential conflicts of interest with respect to the research, authorship, and/or publication of this article.

Acknowledgments

The research is financially supported by National Natural Science Foundation of China (51304209).

Supplementary Materials

"vertical load data. txt" is the time-history curve data of the vertical force measured at the driving test, which is act on the rail to reflect the dynamic stress response at different train speeds. The driving test is divided into three speeds, 80 km/h, 120 km/h, and 160 km/h, respectively. The vertical load data are used as the input load of the simulation model to research the dynamic response of the track under different train speeds. (*Supplementary Materials*)

References

[1] W. Koc, A. Wilk, P. Chrostowski, and S. Grulkowski, "Tests on lateral resistance in railway tracks during the operation of a tamping machine," *Proceedings of the Institution of Mechanical Engineers - Part F: Journal of Rail and Rapid Transit*, vol. 225, no. 3, pp. 325–340, 2011.

[2] D. N. Whittles, S. Kingman, I. Lowndes, and K. Jackson, "Laboratory and numerical investigation into the characteristics of rock fragmentation," *Minerals Engineering*, vol. 19, no. 14, pp. 1418–1429, 2006.

[3] Y. Xu, L. C. Qie, and H. Wang, "Mechanical properties of polyurethane ballast bed based on discrete element method," *J Tongji Univ-Sc*, vol. 47, pp. 1156–1161, 2019.

[4] S. Shao, Y. Yan, and S. Y. Ji, "Discrete-Finite element analysis of dynamic behaviors of ballasted railway with geogrid reinforcement," *China J Solid Mech*, vol. 37, pp. 444–455, 2016.

[5] Y. F. Shi, D. G. Cai, and H. Y. Yan, "Overview on technology of asphalt concrete waterproof sealing layer for high speed railway subgrade," *Railway Engineering*, vol. 58, pp. 33–36, 2018.

[6] G. Saussine, C. Cholet, P. E. Gautier, F. Dubois, C. Bohatier, and J. Moreau, "Modelling ballast behaviour under dynamic loading. Part 1: a 2D polygonal discrete element method approach," *Computer Methods in Applied Mechanics and Engineering*, vol. 195, no. 19-22, pp. 2841–2859, 2006.

[7] L. Liu, S. Y. Song, X. H. Zhang, and Y. Q. Yuan, "Research on dynamic characteristics of asphalt graded crushed stone ballast bed based on discrete element method," *Journal of Physics*, vol. 12, pp. 1–10, 2022.

[8] C. Ergenzinger, R. Seifried, and P. Eberhard, "A discrete element model predicting the strength of ballast stones," *Computers & Structures*, vol. 108-109, pp. 3–13, 2012.

[9] J. F. Ferellec and G. R. McDowell, "A method to model realistic particle shape and inertia in DEM," *Granular Matter*, vol. 12, no. 5, pp. 459–467, 2010.

[10] H. Huang and E. Tutumluer, "Image-aided element shape generation method in discrete-element modeling for railroad ballast," *Journal of Materials in Civil Engineering*, vol. 26, no. 3, pp. 527–535, 2014.

[11] S. Hentz, L. Daudeville, and F. V. Donze, "Identification and validation of a discrete element model for concrete," *Journal of Engineering Mechanics*, vol. 130, no. 6, pp. 709–719, 2004.

[12] X. C. Wang, Z. L. Wang, and Y. P. Huang, "Particle fiow simulation of macro- and meso-mechanical behavior of the prefabricated fractures rock sample," *Hydrogeology & Engineering Geology*, vol. 48, pp. 86–92, 2021.

[13] X. Zhang, C. F. Zhao, and W. M. Zhai, "Discrete element simulation and field test on dynamic behavior of heavy haul railway ballast," *Journal of the China Railway Society*, vol. 41, pp. 169–176, 2019.

[14] X. M. Zhang, X. F. Chen, and Z. P. Zeng, "Experimental study on the quality state parameter of ballast in Qinghai-Tibet railway," *Journal of Railway Science and Engineering*, vol. 4, pp. 64–67, 2007.

[15] Tb 10754-2010, "High-speed railway design code," 2010, https://www.chinesestandard.net/List/TB.aspx/Page3.

[16] Y. Zhuang and K. Y. Wang, "Three-dimensional shakedown analysis of ballasted railway structures under moving surface loads with different load distributions," *Soil Dynamics and Earthquake Engineering*, vol. 100, pp. 296–300, 2017.

[17] X. Zhang, C. F. Zhao, and W. M. Zhai, "Discrete element simulation and its validation on vibration and deformation of railway ballast," *China J Solid Mech*, vol. 38, pp. 1481–1488, 2017.

[18] S. Lobo-Guerrero and L. E. Vallejo, "Discrete element method analysis of rail track ballast degradation during cyclic loading," *Granular Matter*, vol. 8, no. 3-4, pp. 195–204, 2006.

[19] W. Salim and B. Indraratna, "A new elastoplastic constitutive model for coarse granular aggregates incorporating particle breakage," *Canadian Geotechnical Journal*, vol. 41, no. 4, pp. 657–671, 2004.

[20] J. H. Feng and W. M. Yan, "Numerical simulation for train stochastic vibrating loads," *Journal of Vibration and Shock*, vol. 4, pp. 49–53, 2008.

[21] Vertical load date, "In-situ measured data of the driving test - vertical load date.txt," 2022.

[22] X. Xu, Z. Y. Shi, and J. Wieslaw, "Instantaneous frequencies identification of a linear time-varying structure using continuous wavelet transformation of free decay acceleration response," *Journal of Vibration and Shock*, vol. 31, pp. 166–171, 2012.

[23] R. Fu, R. H. Fu, and A. S. Fu, "Composition and amplitude-frequency characteristics of ground motion acceleration based on fast fourier transform analysis," *Acta Seismologica Sinica (English edition6787y7uio])*, vol. 36, pp. 417–424, 2014.